Experimental study on reinforced concrete filled circular steel tubular columns

Wei Hua [1a], Hai-Jun Wang [*1] and Akira Hasegawa [2b]

[1] *College of Architectural Engineering, Shenyang University of Technology, No.111, Shenliao West Road, Economic & Technological Development Zone, Shenyang,110870, P.R. China*
[2] *Dept. of Environmental and Civil Engineering, Hachinohe University of Technology, 88-1 Ohbiraki, Hachinohe 031-8501, Japan*

Abstract.   Experimental results of 39 specimens including concrete columns, RC columns, hollow steel tube columns, concrete filled steel tubular (CFT) columns, and reinforced concrete filled steel tubular (RCFT) columns are presented. Based on the experimental results, the load-carrying capacity, confined effect, ductility, and failure mode of test columns are investigated. The effects of the main factors such as width-thickness ratio (the ratio of external diameter and wall thickness for steel tubes), concrete strength, steel tube with or without rib, and arrangement of reinforcing bars on the mechanical characteristics of columns are discussed as well. The differences between CFT and RCFT are compared. As a result, it is thought that strength, rigidity and ductility of RCFT are improved; especially strength and ductility are improved after the peak of load-displacement curve.

1. Introduction

In recent years, CFT is widely used as a kind of composite structure in the field of engineering works and construction because of its high strength, deformation, toughness and so on. A lot of theses on CFT have been presented up to now (Cao *et al*. 2008, Chung *et al*. 2007, Deng *et al*. 2013, Geng *et al*. 2012, Lu *et al*. 2007, Tao *et al*. 2007, Wang *et al*. 2009, Xu *et al*. 2011, Yang *et al*. 2008, 2010). However, shearing failure of core concrete and local buckling of the steel tube is a huge hidden danger for CFT structures. Inserting steel bars or setting reinforced ribs is effective measures to solve the above problems.

On the other hand, the 1995's Hyogoken-Nanbu earthquake of Japan had caused substantial damage to RC piers (JSCE 1999). The major problems involved in the damaged RC piers were inadequate shear strength and deformation. As a kind of repair measure, steel plane was wrapped around the RC piers, these reinforcement structures can be considered as RCFT structures. Based

---

*Corresponding author, Professor, E-mail: weiflower1973@aliyun.com
[a] Associate Professor, E-mail: wang_navy@hotmail.com
[b] Professor, E-mail: hasegawa@hi-tech.ac.jp

on researches on RCFT until now (Cai and He 2005, Endo *et al*. 2000, Hasegawa *et al*. 2001, Miao 2010, Wang *et al*. 2004, Xiamuxi and Hasegawa 2011), it is understood that filled concrete can be effective to shear force by inserting reinforcing bars and shear failure of filled concrete will not occur. Furthermore, if steel tube with rib is used, unification of steel and concrete will be promoted. Based on those results, it is thought that strength, rigidity and ductility of RCFT are improved; especially strength and ductility are improved after the peak of moment-curvature curve as compared with CFT. In this paper, the outline of compression test, the experimental results and the obtained conclusions are described. The effect of main parameters on mechanical characteristics of RCFT is analyzed clearly.

2. Outline of compression test

2.1 Test specimens and material properties

Fig. 1 and Table 1 show the section size and details of compression test specimens, respectively.
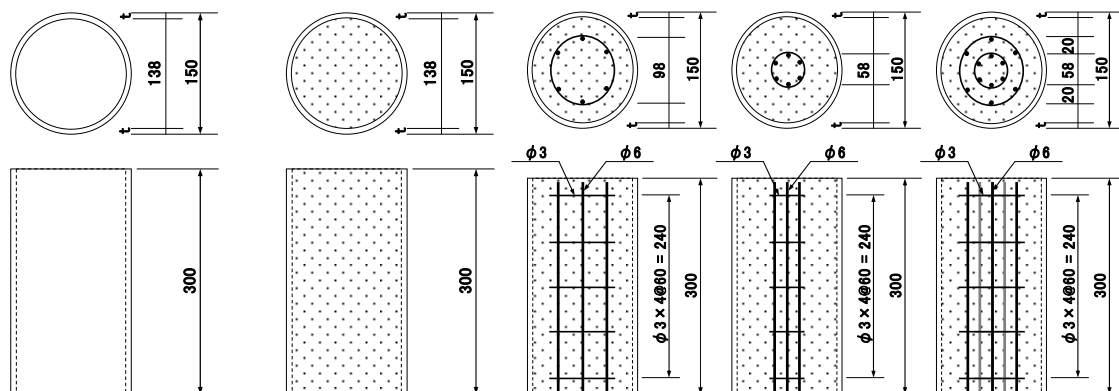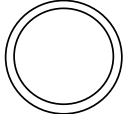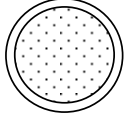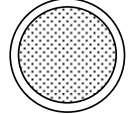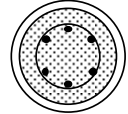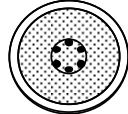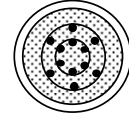

Fig. 1 Column specimens' size (unit: mm)

Table 1 Details of test specimens

Type of specimens	Hollow steel tube	CFT		RCFT with thin cover	RCFT with thick cover	RCFT with double reinforcements
		High strength	Low strength			
RC	- -	CHM-C	CLM-C	CLB-C	CLS-C	CLW-C
3.2 mm	N32CH-C	N32HM-C	N32LM-C	N32LB-C	N32LS-C	N32LW-C
4.5 mm	N45CH-C	N45HM-C	N45LM-C	N45LB-C	N45LS-C	N45LW-C
6.0 mm	N60CH-C	N60HM-C	N60LM-C	N60LB-C	N60LS-C	N60LW-C
6.0 mm (rib)	R60CH-C	R60HM-C	R60LM-C	R60LB-C	R60LS-C	R60LW-C

Fig. 2 Shape of the rib
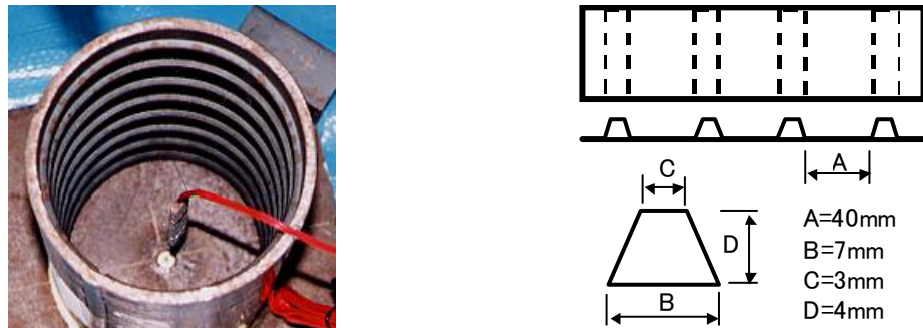
Table 2 Material properties of concrete

Type of concrete	28-day compression strength (N/mm²)	Maximum size of the coarse aggregate (mm)	Water cement ratio (%)	Air content (%)	Fine aggregate content (%)	Proportion (Kg/m³)				Addition (g)
						Water	Cement	Fine aggregate	Coarse aggregate	
High strength	50.0	15	43.5	4.3	51.3	185	425	598 255	837	200
Low strength	19.2	15	64.0	11.0	60.0	190	297	736 316	726	500

According to filling situation, 4 pieces of hollow steel tubes, 8 pieces of CFT and 12 pieces of RCFT specimens were made and tested. Furthermore, 15 pieces of concrete and RC specimens reinforced the same as CFT/RCFT specimens were tested in order to estimate the cumulative strength discussed later. The size of specimens is 150 mm in the diameter, 300 mm in height, and 3.2 mm, 4.5 mm and 6 mm in the thickness of steel tube (see Fig. 1). The ribs are trapezoid with upper bottom of 3 mm, lower bottom of 7 mm and height of 4 mm, which are welded inside steel tubes in circumferential direction per 40 mm (see Fig. 2). Compressive strength of concrete at an age of 28 days was 50.0 N/mm² (high strength) and 19.2 N/mm² (low strength), respectively. The steel tubes were made of mild steel (STK400, Japanese Industrial Standards: JIS). Reinforcing bars were made of SR295 (in JIS). Sizes and arrangement of reinforcing bars are shown as Fig. 1 and Table 1, respectively. Tables 2-3 give the material properties of concrete and steel tubes.

Table 3 Material properties of steel tubes

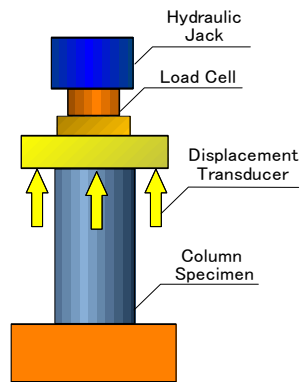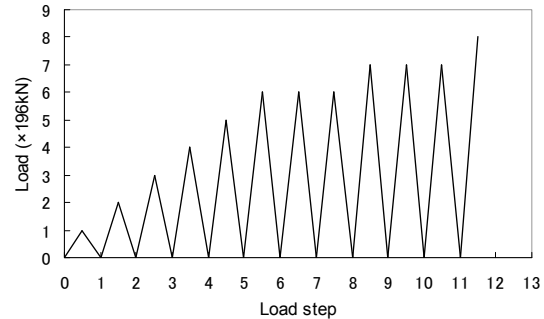| Thickness (mm)	Yield strength (N/mm²)	Tensile strength (N/mm²)
3.2	299	447
4.5	296	462
6	285	459
6 (rib)	285	459

Fig. 3 Test setup of the columns
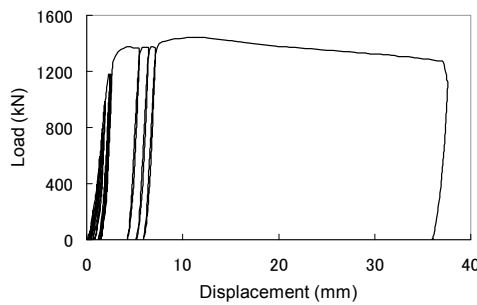

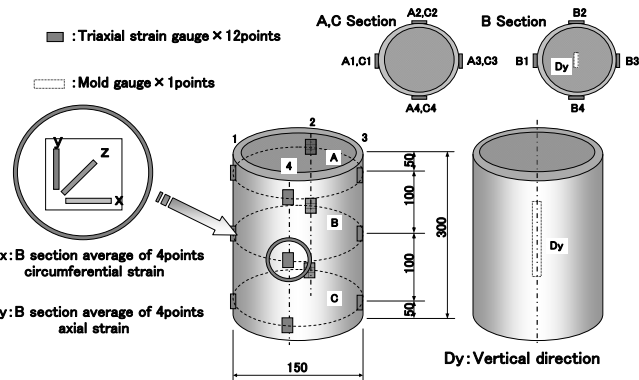Fig. 4 Load step

Fig. 5 Load-displacement curve of N45LW-C

Fig. 6 Details of strain gauges

2.2 Test setup and measurements

A 2940 kN capacity-testing machine shown as Fig. 3 was used in compression test. The upper end of column was free, and the lower end was welded (four points) on the steel plate. The specimens were placed into the testing machine and the cyclic loads were applied on the specimens under load control with load speed of 5.88 kN/sec (0.6 tf/sec). The load increment was 196 kN (20 tf) and 3 times cyclic load was carried out from 1176 kN (120 tf) shown in Fig. 4. Fig. 5 showed an example of RCFT specimen's load-displacement curve according to load step by Fig. 4. The axial deformation was measured for each specimen by 4 displacement transducers (see Fig. 3), and strains in surface of steel tubes were measured by 12 strain gauges. In order to measure the compressive strain of filled concrete, a mold strain gauge was installed inside of concrete (see Fig. 6). All data were recorded automatically by date-log system. After the load reached the maximum value, if the load fell to 80% of the maximum load or any displacement transducers indicated 40 mm, test would be terminated.

2.3 Test results

2.3.1 The maximum compressive strength, confined effect and ductility ratio
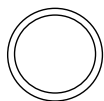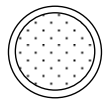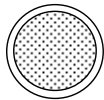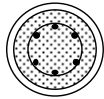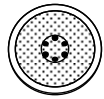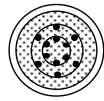
Table 4 gives the maximum compressive strength, confined effect and ductility ratio obtained from the test. The cumulative compressive strength, confined effect is explained as following formulas

$$N_0 = N_c + N_s, \quad \alpha = N_u / N_0 \tag{1}$$

where N_0 is cumulative compressive strength, N_c, N_s and N_u is maximum compressive strength of concrete or RC specimen, hollow steel tube specimen and CFT or RCFT specimen, respectively. α is confined effect. The ductility ratio is given as following equation

$$\mu = \delta_u / \delta_y \tag{2}$$

Table 4 The maximum compressive strength, confined effect and ductility ratio

Concrete strength	Types of specimens	Speci-men label	Maximum compressive strength (kN)	Average (kN)	Cross section shape	Specimen label	Cumulative compre-ssive strength No (kN)	Maximum compre-ssive strength Nu (kN)	Confined effect α	Ductility ratio μ
Hollow steel tube						N32CH-C	-	492	-	3.3
						N45CH-C	-	821	-	3.5
						N60CH-C	-	959	-	5.5
						R60CH-C	-	1079	-	9.7
High strength	CFT	CHM-C	925 920 788	878		N32HM-C	1370	1517	1.11	1.4
						N45HM-C	1698	1966	1.16	1.5
						N60HM-C	1836	1828	1.00	1.8
						R60HM-C	1957	2150	1.10	1.4
Low strength	CFT	CLM-C	392 343 397	377		N32LM-C	869	975	1.12	1.7
						N45LM-C	1197	13.48	1.12	7.5
						N60LM-C	1335	1375	1.03	6.9
						R60LM-C	1456	1571	1.08	8.5
	RCFT with thin cover	CLB-C	398 484 507	463		N32LB-C	955	1052	1.10	4.6
						N45LB-C	1283	1374	1.07	5.6
						N60LB-C	1421	1509	1.06	9.4
						R60-LB-C	1542	1642	1.06	10.5
	RCFT with thick cover	CLS-C	531 478 530	513		N32LS-C	1005	1041	1.04	4.3
						N45LS-C	1333	1369	1.03	5.2
						N60LS-C	1471	1473	1.00	7.6
						R60LS-C	1592	1669	1.05	5.1
	RCFT with double reinforce-ments	CLW-C	484 603 561	549		N32LW-C	1041	1139	1.09	4.5
						N45LW-C	1369	1442	1.05	5.0
						N60LW-C	1507	1565	1.04	7.1
						R60LW-C	1628	1814	1.11	8.2

where μ is ductility ratio; δ_u is displacement at maximum compressive strength and δ_y is yield displacement.

It can be seen from Table 4 that the confined effect of CFT/RCFT specimens with thickness of 3.2 mm is the highest. The reason is that thin steel tube is low resistance against local buckling; filled concrete or RC can generate replenishing effect. The smaller the width-thickness ratio was, the greater maximum compressive strength and ductility ratio would be.

The confined effect of RCFT with double reinforcements is approximately the same as that of RCFT with thin or thick cover. It is considered that arrangement of reinforcing bars has hardly effect on confined effect. The maximum compressive strength of RCFT with thick cover is approximately the same as that of RCFT with thin cover; it is considered that the cover's thickness has little effect on bearing capacity. The ductility ratio of RCFT with thin cover is slightly high than that of RCFT with thick cover.

Figs. 7(a)-(d) show the load-displacement skeleton curve of CFT/RCFT column specimens without ribs (3.2 mm, 4.5 mm, 6.0 mm thick steel tube) and column specimens with ribs respectively. Fig. 8 shows the load-displacement skeleton curve of RCFT columns with double reinforcements.

From Table 4, it can be seen that the maximum compressive strength of CFT column specimens is increased, but ductility ratio is decreased. This appearance can be explained from Fig. 7. The skeleton curve of CFT columns filled with high strength concrete sharply declined after

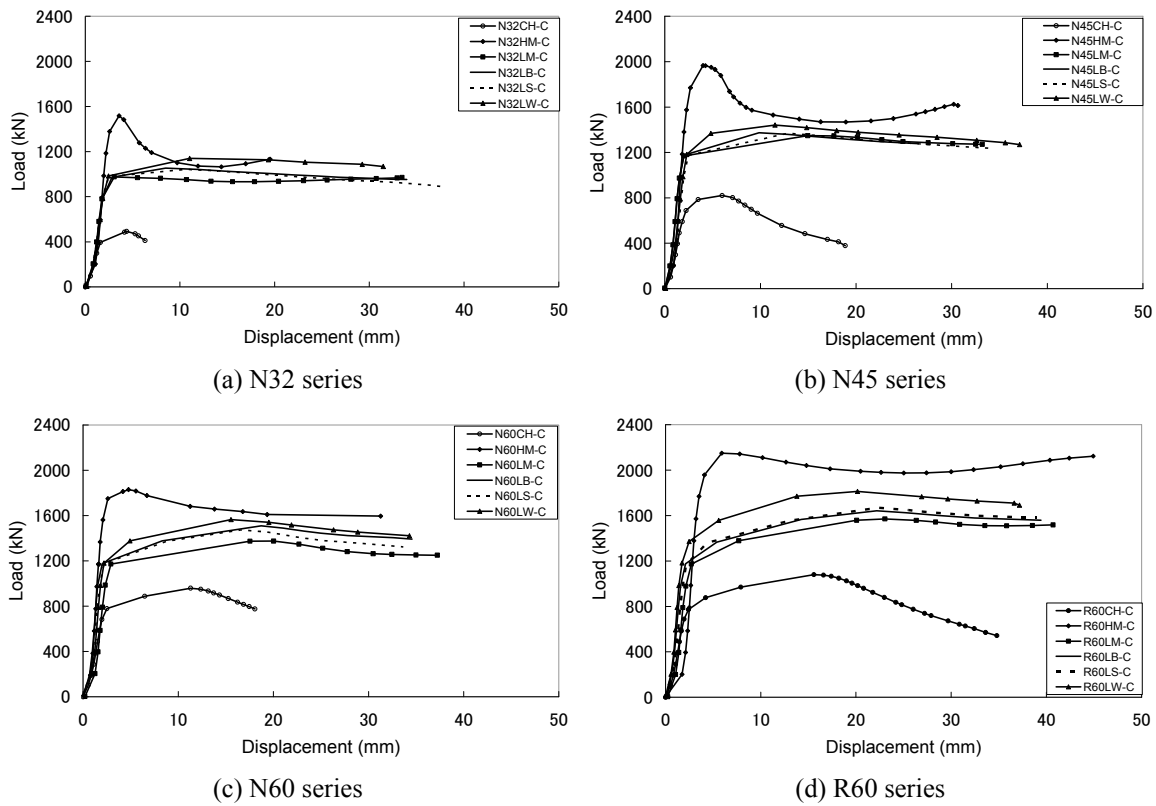(a) N32 series (b) N45 series

(c) N60 series (d) R60 series

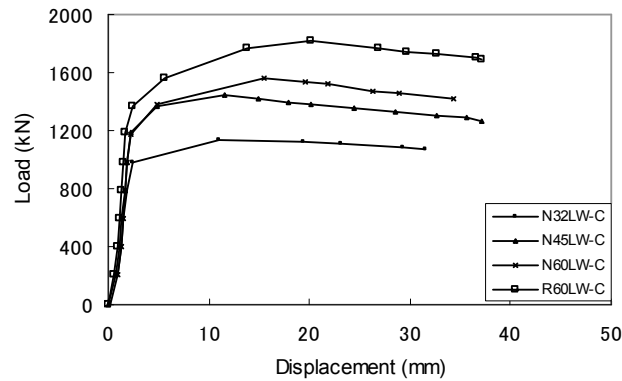Fig. 7 Load-displacement skeleton curves

Fig. 8 Load-displacement skeleton curves for LW-C series

attaining the maximum compressive strength, showed obvious brittle fracture trend, then the compressive strength rose again along with that steel tube showed strong toughness. The thicker the steel tube was, the greater toughness would be. In particular, steel softening degree of CFT columns with ribs was lower after attaining the maximum compressive strength; decreasing degree of bearing capacity was lower. Compared with CFT/RCFT columns filled with high strength concrete, the skeleton curves of CFT/RCFT columns filled with low strength did not sharply decline after attaining the maximum compressive strength, but displacement increased gradually at the same time kept the maximum compressive strength, showed good deformation properties. Among all of columns, RCFT column with double reinforcements and ribs showed the most excellent bearing capacity and deformation performance. RCFT columns with thick cover showed much the same mechanical performance as that of RCFT columns with thin cover, it is considered that the cover's thickness has little effect on mechanical performance. The confined effect of CFT columns filled with high strength concrete was almost same as that of CFT columns filled with low strength concrete. It is considered that concrete strength has only a little effect on confined effect.

From Fig. 8 and Table 4, it can be seen that maximum compressive strength, ductility ratio and confined effect of specimens with rib were higher than that specimens without rib. It is considered that rib can increase the compressive strength of steel tube, and it also can increase the restraint effect of filled concrete, thus unification of steel and concrete will be promoted by using ribs.

2.3.2 The strain situation

Figs. 9(a)-(d) show axial stress-strain skeleton curves of RCFT columns with thick cover, with thin cover and with double reinforcements respectively. In which, ε_y and ε_{dy} is axial strain of steel tube surface and filled concrete center respectively. ε_y is the average value of four points' strain at the B section showed as Fig. 6. From these curves, it can be seen that the axial stress-strain skeleton curves of steel tube and filled concrete showed no difference from initial loading to the maximum loading for RCFT columns, after the maximum loading, the two curves showed inconsistent, finally, the maximum strain of filled concrete was greater than that of steel tube surface. Fig. 9(d) shows axial stress-strain skeleton curves of steel tube and concrete for CFT columns. The two curves showed inconsistent from initial loading, and the consistency of two curves was not as good as that of RCFT columns.

Fig. 10 showed the axial strain-stress skeleton curves of steel tube surface and filled concrete for all of RCFT columns. As shown in the Fig. 10, the thickness of steel tube had great influence on stress-strain skeleton curves of RCFT columns, that is, the maximum stress value and corresponding strain value increased along with the increase of the steel tube's thickness. The skeleton curve of RCFT column with the thickness of 3.2 mm showed the characteristic of elastic

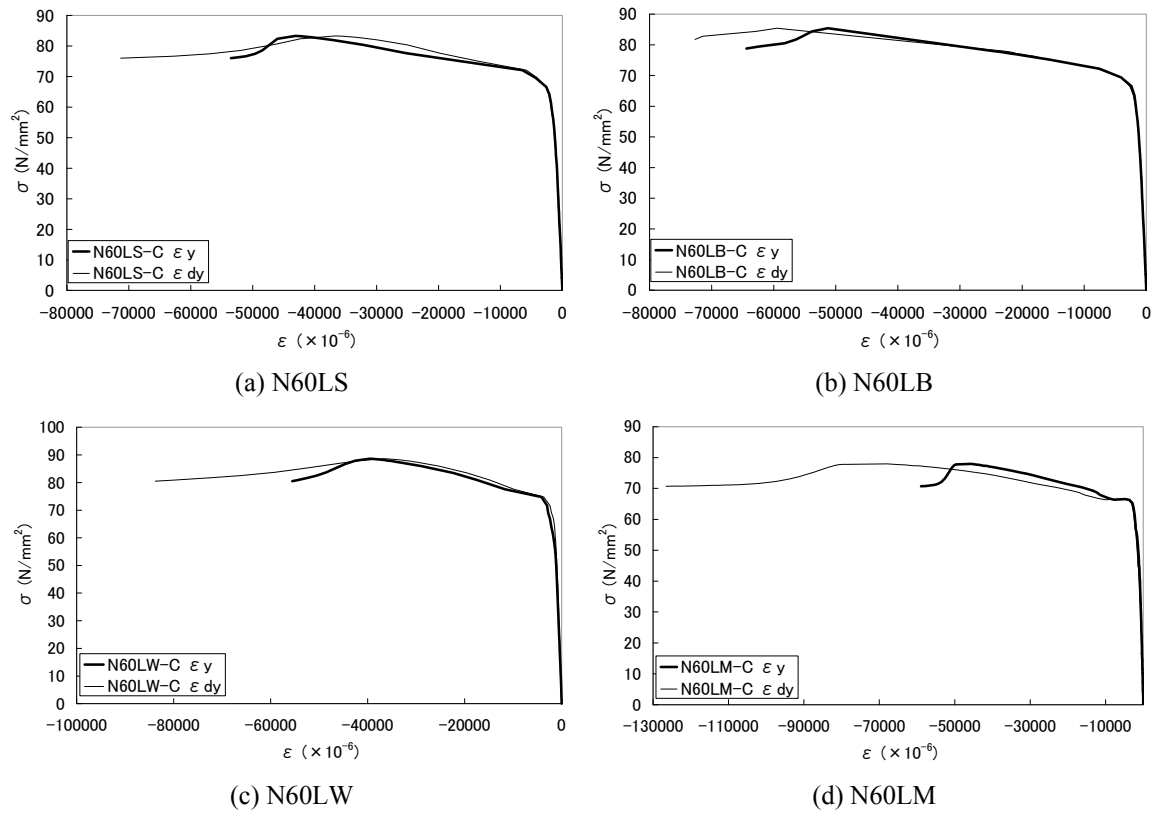

(a) N60LS

(b) N60LB

(c) N60LW

(d) N60LM

Fig. 9 Axial stress-strain skeleton curves of steel tube and filled concrete
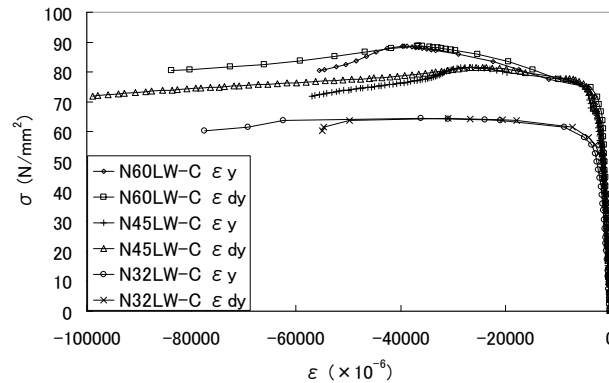

Fig. 10 Axial stress-strain skeleton curves of steel tube and filled concrete for LW series
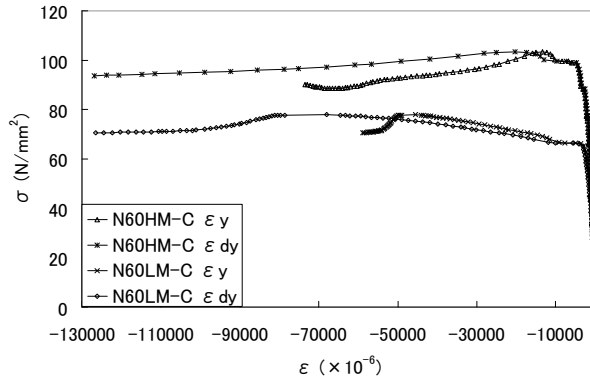
Fig. 11 Axial stress-strain skeleton curves of steel tube and filled concrete for N60HM and N60LM
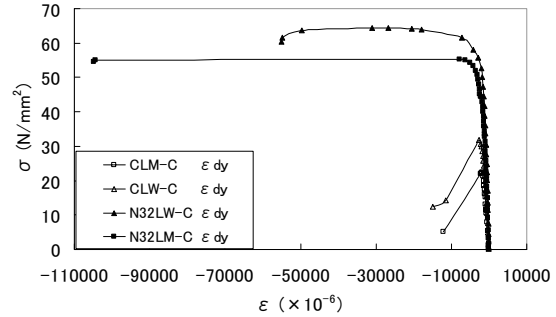
Fig. 12 Axial stress-strain skeleton curves of filled concrete for RC, CFT and RCFT

plastic deformation, in contrast, the curves of RCFT columns with the thickness of 4.5 mm and 6.0 mm presented the slowly rising trend after columns reach yielding, until reaching the maximum value. This phenomenon was very obvious in the case of RCFT columns with the thickness of 6.0 mm. After reaching the maximum value, the strain of steel tube surface and filled concrete decreased slowly respectively. The strain value of filled concrete was greater than that of steel tube surface for RCFT columns with the thickness of 4.5 mm and 6.0 mm.

Fig. 11 shows the axial stress-strain skeleton curves of steel tube surface and filled concrete for CFT columns filled with high strength and low strength concrete. As shown in the Fig. 7(c), for CFT columns filled with high strength, the stress of steel tube surface reached the maximum value at the moment of small strain, and then the stress sharply decreased. But the stress of filled concrete did not sharply decrease.

Fig. 12 shows the axial stress-strain skeleton curves of filled concrete center for concrete column, RC column with double reinforcements, CFT and RCFT columns with double reinforcements and the thickness of 3.2 mm. In the case of concrete column and RC column, the stress sharply decreased to 0 after the stress reached the maximum value. For the corresponding CFT and RCFT columns, the stress did not reduce after the maximum stress reached more than 2 times of concrete and RC columns' maximum stress, at the same time, the strain increased by a wide margin.

Figs. 13(a)-(d) show the relationship between the axial strain ratio of filled concrete center and steel tube surface $\varepsilon_{dy}/\varepsilon_y$ and normalized load ratio P/P_{max} for CFT and RCFT columns. In these Figures, the nearer to 1.0 the strain ratio was, the more obvious the integration of behavior between concrete and steel tube would be.

Fig. 13(a) is the relationship between the axial strain ratio $\varepsilon_{dy}/\varepsilon_y$ and normalized load ratio P/P_{max} of CFT columns filled with low strength concrete. In the case of CFT columns, the axial strain ratio was far away from 1.0 at initial loading, as normalized load ratio P/P_{max} grew, the strain ratio gradually close to 1.0. The integration of behavior between concrete and steel tube was weak. The thicker the steel tube was, the more obvious the tendency would be. This tendency could be improved by using ribs for columns, columns with ribs showed obvious integration of behavior.

Figs. 13(b)-(c) are the relationship between the axial strain ratio $\varepsilon_{dy}/\varepsilon_y$ and normalized load ratio

P/P_{max} of RCFT columns with thick cover and double reinforcements respectively. It can be found that the axial strain ratio was gradually near to 1.0 from initial loading; the integration of behavior of steel tube and concrete was obvious. The thicker the steel tube was, the higher the integration degree would be.

Fig. 13(d) is the relationship between the axial strain ratio $\varepsilon_{dy}/\varepsilon_y$ and normalized load ratio P/P_{max} of N60 columns series. It can be seen that the quantity and arrangement location of reinforcing bars had small influence on the integration of behavior.

In general, the Poisson ratio of steel tube and concrete is approximately 0.3 and 0.2 respectively in the elastic region for compressive CFT/RCFT columns. The steel tube has hardly confinement effect on filled concrete when steel tube and concrete is simultaneously compressed. But filled concrete expands along the circumferential direction toward steel tube once entering the plastic region; concrete's deformation is larger than that of steel tube. That is to say, filled concrete is in the triaxial stress state because of the confinement effect caused by circumferential strain difference between filled concrete and steel tube, and its compressive bearing capacity increases by a wide margin. The confinement effect will be analyzed as following based on the variation state of circumferential strain to axial strain ratio (Poisson ratio) of steel tube and filled concrete along with the loading.

The relationship of circumferential strain ε_x and axial strain ε_y of steel tube surface is shown as Figs. 14(a)-(d) for hollow steel tube, low strength CFT, RCFT with double reinforcements and

(a) LM series
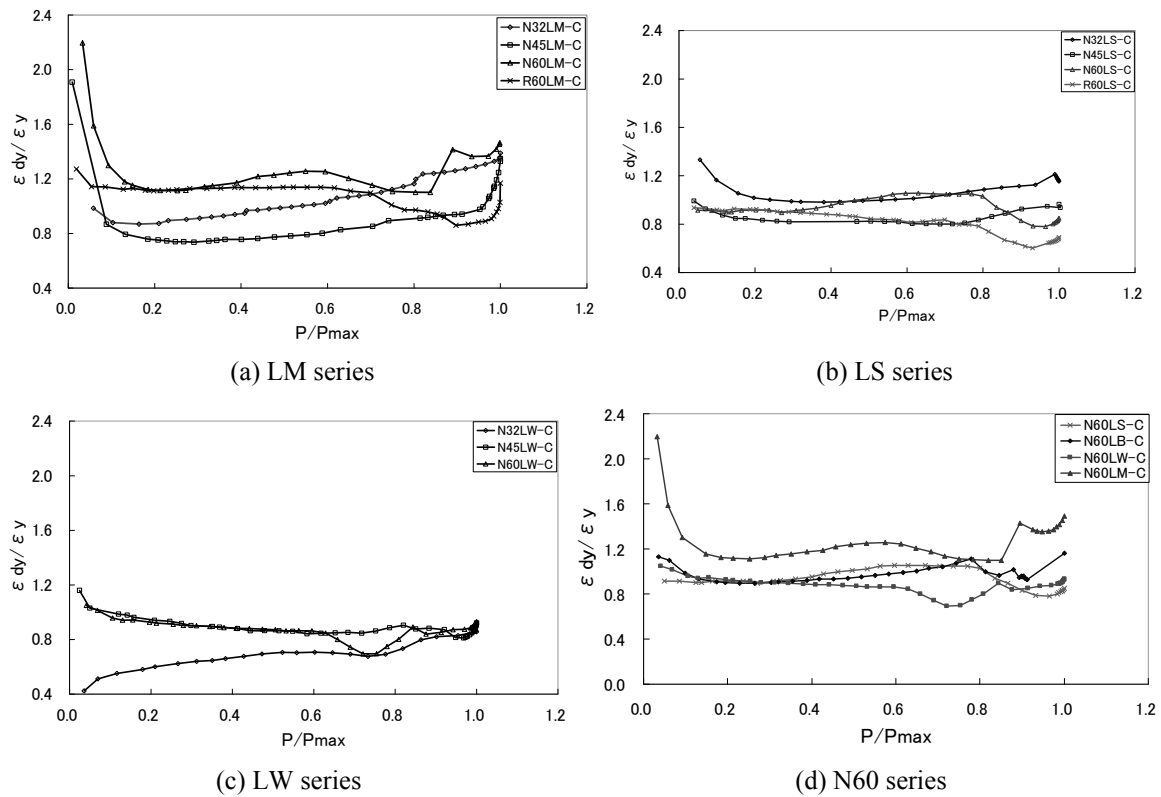
(b) LS series

(c) LW series

(d) N60 series

Fig. 13 Relationship between $\varepsilon_{dy}/\varepsilon_y$ and P/P_{max}

(a) CH series

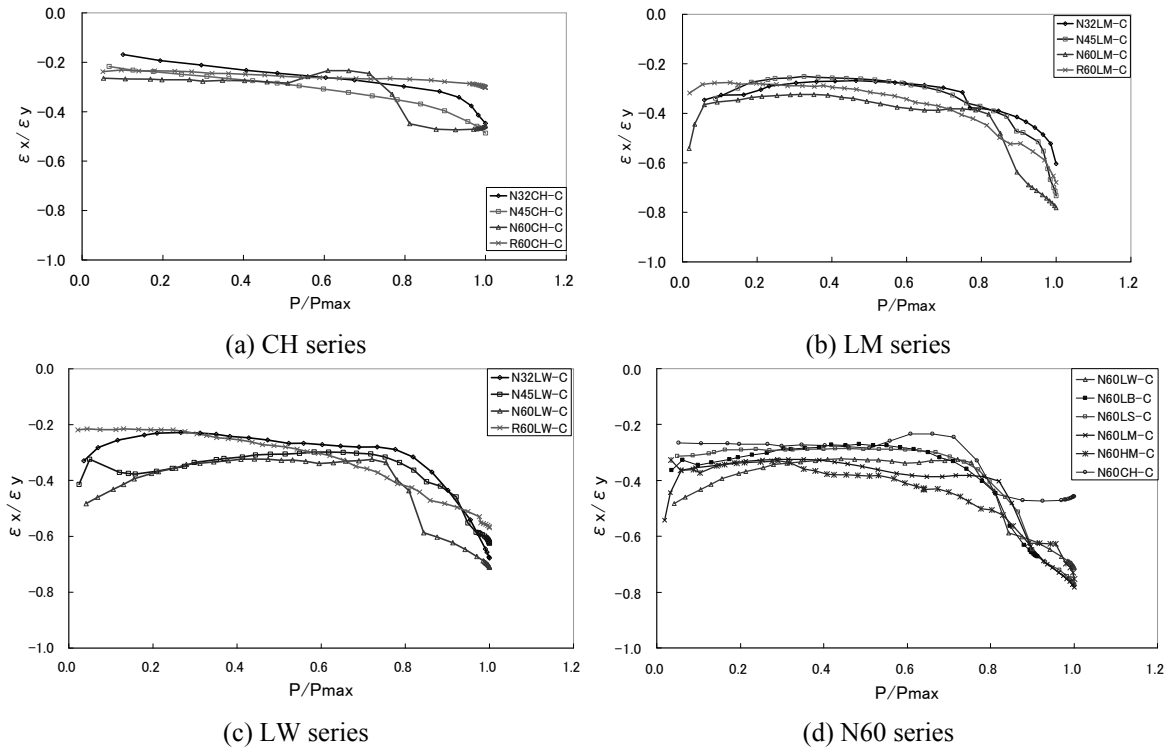(b) LM series

(c) LW series

(d) N60 series

Fig. 14 Relationship between $\varepsilon_x/\varepsilon_y$ and P/P_{max}

N60 series columns. The longitudinal axis expresses the ratio ($\varepsilon_x/\varepsilon_y$) of circumferential direction strain to axial strain of steel tube surface, and the horizontal axis represents normalized load ratio (P/P_{max}). The absolute value of the strain ratio represented by longitudinal axis is the Poisson's ratio.

Fig. 14(a) steel tube columns. In the case of 3.2 mm and 4.5 mm thick hollow steel tube columns without ribs, the strain ratio is the relationship between the strain ratio of steel tube surface and normalized load ratio for hollow changed from -0.2 to -0.3 from initial loading, it slowly began to decline after the load ratio reached 0.6, and it reached -0.5 when normalized load ratio reached 1.0. In contrast, for 6.0 mm thick hollow steel tube column without ribs, the strain ratio sharply began to decline from -0.3 when normalized load ratio approximately reached 0.7, and it kept about -0.5 after normalized load ratio reached 0.8. For 6.0 mm thick hollow steel tube column with ribs, the strain ratio slowly declined from -0.2 to -0.3, and it did not sharply decline before reaching the maximum bearing capacity.

Fig. 14(b) is the relationship between the strain ratio of steel tube surface and normalized load ratio for CFT columns filled with low strength concrete. For low strength CFT columns with the thickness of 3.2 mm shown as Fig. 14(b), the strain ration changed near to -0.3 when normalized load ratio changed from 0.0 to 0.7, hereafter, it sharply declined, and it reached -0.6 when load ratio reached 1.0. The variation situation of strain ratio along with load ratio for CFT columns with the thickness of 4.5 mm was basically similar to that of CFT columns with the thickness of 3.2 mm, however, it reached -0.75 when load ratio reached 1.0. In the case of CFT columns with the

thickness of 6.0 mm, the strain ratio sharply raised from -0.55 to -0.35 when load ratio changed from 0.0 to 0.05, then it varied near to -0.35 until load ratio reached 0.8, hereafter, it sharply declined, and it reached -0.8 when load ratio reached 1.0. Therefore, filled concrete strength had great influence on the confinement effect of CFT columns in initial loading and after the stage of load ratio reaching 0.7.
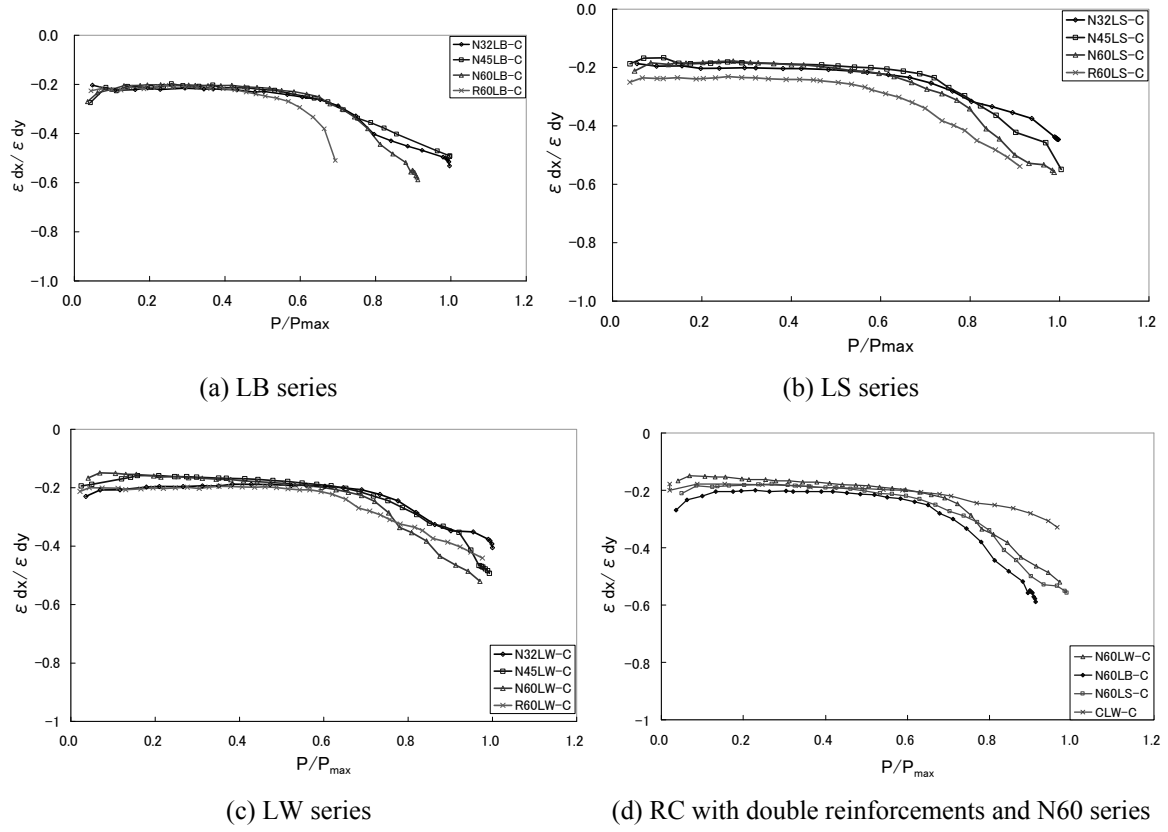
Fig. 14(c) is the relationship between the strain ratio of steel tube surface and normalized load ratio for RCFT columns with double reinforcements. For columns with the thickness of 3.2 mm, the strain ratio slowly rose from -0.35 to -0.25 when the load ratio varied from 0.0 to 0.25, then it slowly declined, it was -0.3 when the load ratio reached 0.75, hereafter, it sharply declined, and it reached -0.7 when the load ratio reached 1.0. For columns with the thickness of 4.5 mm, the strain ratio slowly varied from -0.4 to -0.3 when the load ratio varied from 0.1 to 0.7, then it sharply declined, and it was -0.65 when the load ratio reached 1.0. The variation situation of strain ratio along with load ratio for RCFT columns with the thickness of 6.0 mm was basically similar to that of RCFT columns with the thickness of 4.5 mm. The declining degree of the strain ratio was greater than that of RCFT columns with the thickness of 4.5 mm after the load ratio reached 0.75, and it was -0.7 when the load ratio reached 1.0.

Fig. 14(d) is the relationship between the strain ratio of steel tube surface and normalized load ratio for hollow steel tube columns, CFT and RCFT columns with the thickness of 6.0 mm. In the case of RCFT and CFT columns filled with low strength, the strain ratio varied from -0.3 to -0.4 when the load ratio varied from 0.0 to 0.7-0.8, then it sharply declined. In contrast, for hollow steel tube columns, the strain ratio changed near to -0.3 when the load ratio changed from 0.0 to 0.6, then it sharply declined to -0.5 when the load ratio was 0.6-0.8, hereafter, it varied near to -0.5. It can be seen that the ratio of circumferential direction strain to axial strain of steel tube surface (Poisson ratio) for CFT/RCFT columns increased as compared with hollow steel tube columns because that filled concrete expanded towards circumferential direction of steel tube after the concrete entering into the plastic region.

The above discussed the strain ratio of steel tube surface; the variation situation about strain ratio of filled concrete for RCFT columns was analyzed as follows. Figs. 15(a)-(c) are the relationship between circumferential direction strain and axial strain of filled concrete for RCFT columns with thin cover, thick cover and double reinforcements. The longitudinal axis expresses the ratio ($\varepsilon_{dx}/\varepsilon_{dy}$) of circumferential direction strain to axial strain of filled concrete, and the horizontal axis represents normalized load ratio ($P/P_{\max}$).

The thickness of steel tube had little influence on the strain ratio of filled concrete in the case of RCFT columns with thin cover shown as Fig. 15(a). The strain ratio changed near to -0.2 when the load ratio changed from 0.0 to 0.4, then it slowly declined, it was -0.5 (for RCFT columns with the thickness of 3.2 mm and 4.5 mm) and -0.6 (for RCFT columns with the thickness of 6.0 mm) respectively when the load ratio reached 1.0. For ribbed RCFT columns with thin cover and the thickness of 6.0 mm, the variation situation of strain ratio was same as that of corresponding non-ribbed RCFT columns. The strain ratio sharply declined after the load ratio reached 0.4, and it was -0.5 when the load ratio reached 0.7, the test was terminated.

The thickness of steel tube had little influence on the strain ratio of filled concrete in the case of RCFT columns with thick cover shown as Fig. 15(b). The strain ratio changed near to -0.2 when the load ratio changed from 0.0 to 0.5, then it slowly declined, it was -0.5 when the load ratio reached 1.0. For ribbed RCFT columns with thick cover and the thickness of 6.0 mm, the strain ratio changed near to -0.25 when the load ratio varied from 0.0 to 0.5, hereafter, it slowly declined, and the variation situation of strain ratio was same as that of corresponding non-ribbed RCFT

(a) LB series

(b) LS series

(c) LW series

(d) RC with double reinforcements and N60 series

Fig. 15 Relationship between $\varepsilon_{dx}/\varepsilon_{dy}$ and $P/P_{\max}$

columns.

The thickness of steel tube had little influence on the strain ratio of filled concrete in the case of RCFT columns with double reinforcements shown as Fig. 15(c). The strain ratio changed near to -0.2 when the load ratio changed from 0.0 to 0.6, then it slowly declined after the load ratio reached 0.5, and it was -0.4 ~ -0.55 when the load ratio reached 1.0.

Fig. 15(d) is the relationship between the ratio $\varepsilon_{dx}/\varepsilon_{dy}$ of circumferential direction strain to axial strain of filled concrete and normalized load ratio $P/P_{\max}$ for double reinforced concrete columns and RCFT columns with the thickness of 6.0mm. The strain ratio varied near to -0.2 when the load ratio varied from 0.0 to 0.6, then it slowly declined, and all of curves showed the same tendency. The strain ratio was in the range of -0.5 ~ -0.6 for RCFT columns with double reinforcements when the load ratio reached 1.0, however, it was -0.3 for double reinforced concrete columns.
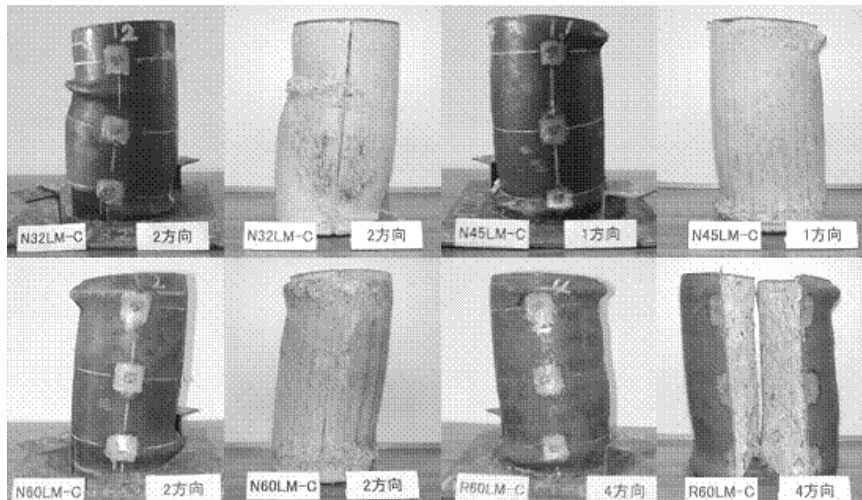
2.3.3 Failure mode

Figs. 16(a)-(f) show the failure mode of columns specimens' inside and outside. Local buckling was observed at lower end of column in hollow steel tube specimens. For 6.0 mm thick hollow steel tube specimen, local buckling occurred at both upper and lower end. Almost all of the CFT/RCFT specimens occurred local buckling along slant direction from the upper to the lower end of steel tube. For CFT/RCFT column specimens with thickness of 3.2 mm, local buckling also

occurred at the middle of the steel tube. After testing, steel tube of typical specimens were cut and removed to make sure of the failure mode of filled concrete. Concrete were crushed at the part of steel tube occurred local buckling, and there were not penetrable cracks, no serious crush occurred. In the case of CFT and RCFT specimens with rib, the phenomenon that the coating of the surface of steel tube flaked off in the rib pattern was seen; steel tube and concrete could not be absolutely separated. It is considered that unification of steel and concrete would be promoted if steel tube with rib was used.
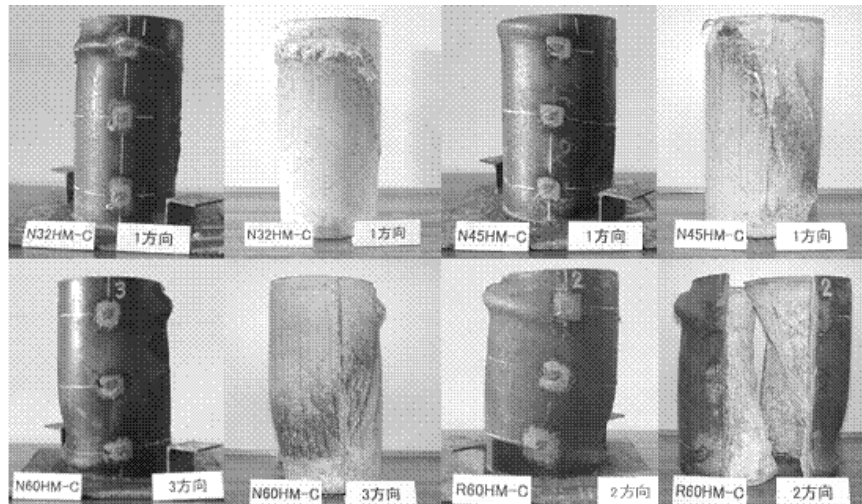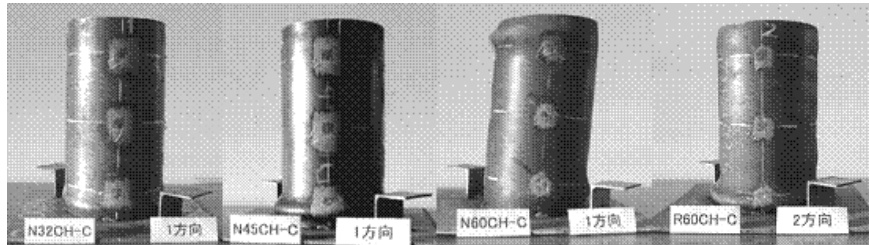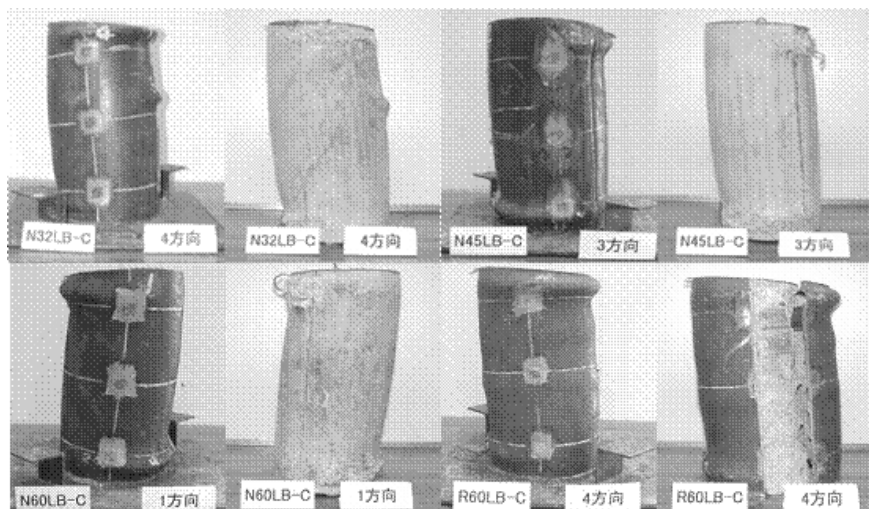

(a)

(b)

Fig. 16 (a) Failure mode of CFT columns filled with high strength concrete; (b) Failure mode of CFT columns filled with low strength concrete; (c) Failure mode of hollow steel tube columns; (d) Failure mode of RCFT columns with double reinforcements; (e) Failure mode of RCFT columns with thin cover; (f) Failure mode of RCFT columns with thick cover
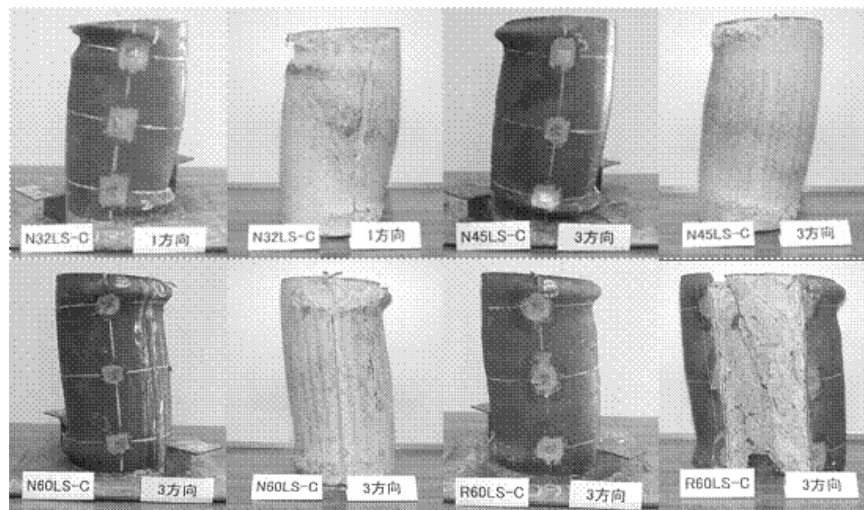
(c)

(d)

(e)

Fig. 16 Continued

(f)

Fig. 16 Continued

3. Conclusions

In this study, rib-less steel pipes and ribbed steel pipes were used, compression test was carried out. From the experimental results, the following conclusions can be drawn.

- CFT filled with high strength concrete shows higher maximum compressive strength, but ductility ratio is lower than that of other specimens. The confined effect of CFT columns filled with high strength concrete is almost same as that of CFT columns filled with low strength concrete. It is considered that concrete strength has only a little effect on confined effect. CFT columns filled with high strength concrete rapidly lost strength after the maximum compressive strength, and showed the brittle fracture trend, this trend is especial apparent for the columns with great width-thickness ratio.
- In the case of RCFT columns, shear failure of filled concrete doesn't occur after inserting reinforcing bars; reinforcements can effectively increase the shear bearing capacity of columns. RCFT columns show more excellent compression bearing capacity and deformation performance than hollow steel tube and CFT columns. Compared with CFT columns, RCFT columns indicate better integration performance of steel tubes and filled concrete from the initial loading.
- After steel tubes are ribbed, the integration performance of steel tubes and filled concrete is promoted, and the compression bearing capacity is raised. When columns are failure, filled concrete and steel tubes are inseparable, and the ductility of columns is enhanced.
- The greater the width-thickness ratio is, the better confined effect on filled concrete would be, filled concrete can more effectively resist against local buckling of steel tubes.

References

Cai, J. and He, Z.Q. (2005), "Axial load behavior of square CFT stub column with binding bars", *J. Constr. Steel Res.*, **62**(5), 472-483.

Cao, W.L., Wang, M., Zeng, B. and Zhang, J.W. (2008), "Seismic experimental research of concrete filled steel tube columns-concrete composite shear wall", *Proceedings of the 14th World Conference on Earthquake Engineering*, Beijing, China, October.

Chung, K.S., Chung, J.A. and Choi, S.M. (2007), "Prediction of pre- and post-peak behavior of concrete filled square steel tube columns under cyclic loads using fiber element method", *Thin-Wall. Struct.*, **45**(9), 747-758.

Deng, Z.C., Wang, Y.J., Zhang, X.D., Huang, Y. and Liu, X.C. (2013), "Axial compression performance of IHFRP confined concrete column", *J. Shenyang Univ. Technol.*, **35**(2), 218-223.

Endo, T., Shioi, Y., Hasegawa, A. and Wang, H.J. (2000), "Experimental study on reinforced concrete filled steel tubular structure", *Proceeding of 7th International Conference on Steel and Space Structures*, Singapore, May.

Geng, Y., Wang, Y.Y. and Zhang, S.M. (2012), "Time-dependent behavior of concrete-filled steel tubular columns: analytical and comparative study", *Mag. Concr. Res.*, **64**(1), 55-69.

Hasegawa, A., Shioi, Y., Wang, H.J., Endo, T. and Isibashi, H. (2001), "Experimental study on mechanical characteristics of reinforced concrete filled steel tubular structures", *Proceedings of the First International Conference on Steel and Composite Structures*, Pusan, Korea, June.

JSCE (1999), *Reality State and Analysis of Steel Construction Damaged by Hansin-Awaji Earthquake*, Japan Society of Civil Engineers, Tokyo, Japan.

Lu, X.L., Li, X.P. and Wang, D. (2007), "Modeling and experimental verification on concrete-filled steel tubular columns with L or T section", *Front. Archit. Civil Eng. China*, **1**(2), 163-169. [In English]

Miao, W. (2010), "Experimental research and bearing capacity analysis of axially compressive reinforced concrete-filled steel tube short column", *Shanxi Archit.* (*in Chinese*), **36**(5), 79-81.

Tao, Z.H., Han, L.H. and Wang, D.Y. (2007) "Experimental behavior of concrete-filled stiffened thin-walled steel tubular columns", *Thin-Wall. Struct.*, **45**(5), 517-527.

Wang, H.J., Hasegawa, A. and Shioi, Y. (2004), "Experimental Study on Mechanical Performances of Reinforced Concrete Filled Square Steel Tubular Structures", *Proceedings of the Third International Conference on Advances in Structural Engineering and Mechanics* (*ASEM'04*), Seoul, Korea, September.

Wang, Y.Y., Yang, Y.L., Zhang, S.M. and Liu, J.P. (2009), "Seismic behaviors of concrete-filled T-shaped steel tube columns", *Key Eng. Mat.*, **400-402**, 677-683.

Xiamuxi, A. and Hasegawa, A. (2011) "Compression test of RCFT columns with thin-walledsteel tube and high strength concrete", *Steel Compos. Struct.*, *Int. J.*, **11**(5), 391-402.

Xu, M., Zhang, S.M., Guo, L.H. and Wang, Y.Y. (2011), "Progressive collapse analysis of concrete-filled steel tubular frames with semi-rigid connections", *Trans. Tianjin Univ.*, **17**(6), 461-468. [In English]

Yang, J.J., Xu, H.Y. and Peng, G.J. (2008), "Behavior of concrete-filled double skin steel tubular columns with octagon section under axial compression", *Front. Archit. Civil Eng. China*, **2**(3), 205-210. [In English]

Yang, Y.L., Yang, H. and Zhang, S.M. (2010), "Compressive behavior of T-shaped concrete filled steel tubular columns", *Int. J. Steel Struct.*, **10**(4), 419-430.

CC